Published by :
https://www.ijert.org/
An International Peer-Reviewed Journal

International Journal of Engineering Research & Technology (IJERT)
ISSN: 2278-0181
Vol. 15 Issue 05 , May - 2026

Artificial Hummingbird Algorithm Optimized Cascaded Tilt Fractional-Order Integral Derivative with Proportional Integral Controller for Harmonic Mitigation in 31-Level Photovoltaic-Fed Multilevel Inverter

[*1a,b]P V V Raghava Sharma,
[*1a]Research Scholar,
Visvesvaraya Technological University,
Belagavi & Research Centre, Guru Nanak Dev Engineering College,
Bidar, Karnataka 585403, India.
[b]Assistant Professor,
Department of Electrical and Electronics Engineering,
MVSR Engineering College,
Hyderabad, Telangana 501510, India.

[2]Dr. Neelashetty K
[2]Professor,
Department of Electrical and Electronics Engineering,
Dept, Member IEEE,
Guru Nanak Dev Engineering College,
Bidar, Karnataka 585403, India.

Abstract: A new method for harmonic reduction in a single-phase 31-level asymmetrical cascaded H-bridge (CHB) multilevel inverter fed by a photovoltaic (PV) source using Artificial Hummingbird Algorithm (AHA) is proposed in this paper. The proposed method utilizes an AHA optimized cascaded tilt fractional-order integral derivative with proportional integral (C-TFOID-PI) controller, which can enhance the harmonic suppression and system stability in the outer side of the loop, and reduce the steady-state tracking error and achieve good output regulation in the inner side of the loop. The optimization technique employed is the Artificial Hummingbird Algorithm (AHA) to optimize all the seven parameters of the controller which are tilt coefficient (K_t)fractional integral order (λ), fractional derivative order (μ), integral gain (K_i)derivative gain $(K_d)$and the PI controller gains $(K_p$ and $K_{i2})$AHA is a bio-inspired meta-heuristic algorithm inspired by hummingbirds' foraging nature (guided, territorial and migratory). Two additional refinements to the algorithm are provided: a nectar refilling process and a visit-table memory system for enhanced convergence speed and prevention of the algorithm from falling into local optimal false conclusions during optimization. Detailed

MATLAB/Simulink simulations of the proposed AHA-based C-TFOID-PI controller are performed and the performance of the controller are verified by some asymmetrical, 31-level multilevel half-bridge inverter (MLI) with asymmetric DC source ratios of 1:2:4:8. The system is tested under standard operating conditions 1000W/m² irradiance, 25°C temperature and under different irradiance conditions. Based on the above simulation findings, the proposed controller outperforms the Green Anaconda Optimization Algorithm (GAOA) based C-TFOID-PI controller in terms of total harmonic distortion (THD) and efficiency as well as convergence rate which is 23.6% faster. Furthermore, the controller meets the IEEE 519-2014 harmonic standard and has superior overall performance compared to traditional PI, PID, FOPID and TFOID-PI controllers.

Keywords—Artificial Hummingbird Algorithm; Cascaded H-bridge multilevel inverter; C-TFOID-PI controller; Fractional-order control; Harmonic mitigation; Photovoltaic system; Total harmonic distortion; Meta-heuristic optimization.

I. INTRODUCTION

Photovoltaic (PV) systems are increasingly becoming a key tool in global efforts to transition to clean and sustainable energy sources due to their advantages. Photovoltaics (PV) are increasingly identified as a critical part of today's global trend towards clean and sustainable energy because of their many benefits. As PV installations keep proliferating in a utility network, requests for efficient and high-performance power electronic interfaces, that are able to generate sinusoidal voltage with minimum harmonic distortion, is growing significantly [1]. In such applications, for medium and high current (power) range grid connected PV application multilevel Inverters (MLI) have emerged as a suitable

International Journal of Engineering Research & Technology (IJERT)
ISSN: 2278-0181
Vol. 15 Issue 05 , May - 2026

solution. In comparison with common 2-level inverter, MLIs have some critical benefits like low voltage stress on the switching devices, low electromagnetic interference (EMI) and improved output voltage waveform quality [2]. The asymmetrical cascaded H-bridge (CHB) topology has drawn considerable interest since it offers more output voltage levels compared to the symmetrical designs with fewer number of DC sources [3]. A near-sinusoidal output with inherently low THD can be seen achievable for a 31-level asymmetrical CHB-MLI based on 4 H-bridge cells operating in different DC voltage ratios: 1:2:4:8. Although these are some benefits of grid connected applications, there are strict compliance measures required for power quality. The IEEE Standard 519-2014 sets a limit for PCC connected systems at 5% voltage total harmonic distortion (THD) [4].

An advanced closed-loop control techniques other than conventional PI and PID controllers is needed to maintain THD below 5% under variable irradiance, temperature changes and dynamic loading condition [5]. Traditional integer order controllers are ineffective in suppressing high frequency harmonics, and exhibit minimum sensitivity to the parameter variations in PV systems. They also lose performance in the case of nonlinear load disturbances [6]. Many of these disadvantages are corrected by the fractional order (FO) control which involves the use of the non-integer integration and differentiation operators. Such an approach provides a greater tuning flexibility, and permits the more accurate tuning of the phase and gain response properties of the system [7].

The Tilt Fractional-Order Controller with Integral Perspective (TFOID) is an enhanced fractional order controller technique which also contains a tilt component to boost the phase margin and thus increase the low-frequency disturbance rejection when compared with the conventional FOPID controller [8]. A cascaded control structure is obtained by stacking a TFOID outer voltage loop with a PI inner current loop and this is called the C-TFOID-PI controller. This control structure was applied in a 31-level PV-fed CHB-MLI system recently. With parameter tuning by the Green Anaconda Optimization Algorithm (GAOA), the controller managed to obtain THD of 0.41% [3]. Although this has increased the number of parameters, two major disadvantages of the GAOA approach were still reported in the study: the slow convergence due to the optimization of several controller parameters and poor performance under dynamic load conditions [3]. The challenges demonstrate the need for an improved optimization strategy.

Recently, an innovative optimization algorithm called Artificial Hummingbird Algorithm (AHA) introduced in 2022 by Jun Zhao, Lidong Wang, and Seyedali Mirjalili [14] has been inspired by the nature of hummingbirds feeding. The algorithm comprises three search strategies: guided foraging, to share information between geographically adjacent agents; territorial foraging, to find local solutions (information and exploitation); and migratory foraging, to locally search and explore the best solution available in the whole area. Aha allows hummingbirds to have a memory of their searches when they visit a table. When added to the food refilling for depleted food when it is exhausted, this population diversity is useful and when convergence occurs it occurs slowly during the optimization process. Because of these properties, AHA is well suited to solving complex high dimensional optimization problems such as the simultaneous tuning of many of the parameters in the C-TFOID-PI controller.

In this paper, for the first time, the Artificial Hummingbird Algorithm (AHA) is proposed to optimize the C-TFOID-PI controller for a 31 level asymmetrical PV-fed CHB-MLI system. The performance analysis of the proposed AHA-based controller is done via MATLAB/Simulink simulation and compared with the comparison of the GAOA-based C-TFOID-PI controller method [3] and a conventional PI, PID, FOPID and TFOID-PI controllers under standard operating condition and dynamic operating condition. The key contributions of this is summarized below:

(i) A new AHA optimization scheme based on the multi-objective equation synthesis method is designed for the simultaneous tuning of all seven parameters of the C-TFOID-PI controller for the optimized optimization structure of a 31-level asymmetrical CHB-MLI system. To our knowledge, this is the first attempt for determining the C-TFOID-PI family of controllers to an HV MLI using AHA.

(ii) A thorough study of AHA's convergence behavior is offered within the C-TFOID-PI parameter space, presenting 23.6% higher convergence performances over GAOA-based approach, as well as under different irradiance and dynamic load conditions.

A detailed comparative study is conducted with five benchmark controllers namely, PI, PID, FOPID, TFOID-PI, GAOA based C-TFOID-PI. Comprehensive comparison of key performance figures like THD, efficiency, conduction and switching losses and dynamic response characteristics.

(vi) The proposed controller meets the overall requirements of the IEEE 519 2004 harmonic standard that states a THD of less than 5%.(iv) The proposed controller is fully compliant with the IEEE 519-2014, which sets the maximum THD at less than 5% for the standard operating conditions of PV modules – 1000 W/m2 Irradiance and Ambient temperature of 25° C.

The rest of the paper is structured as follows. Literature Survey has been put in Section 2. The general system model, including the PV module and the 31-level CHB-MLI configuration, are presented in section 3. The structure and the derivation of the transfer-function of the C-TFOID-PI controller are discussed in section 4. The Artificial Hummingbird Algorithm and its implementation in the optimization of controller parameters are presented in Section 5. A comparative performance analysis and the simulation results are given in Section 6. Lastly, Section 7 concludes the chapter with a summary of the main results of the study and some suggestions for future research.

II. LITERATURE REVIEW

The literature review was conducted under 4 major research fields: multilevel inverter (MLI) topologies and harmonic reduction techniques, design of fractional-order controllers, Artificial Hummingbird Algorithm and Meta-heuristic optimization approaches in power electronics.

Multilevel inverter topologies and Harmonic mitigation.

International Journal of Engineering Research & Technology (IJERT)
ISSN: 2278-0181
Vol. 15 Issue 05 , May - 2026

K. Prabaharan and K. Palanisamy [1] have given a detailed review of reduced switches multilevel inverter (MLI) topologies, which actually showed that the asymmetrical cascaded H-bridge (CHB) MLIs generally offer lower THD than do diode-clamped and flying-capacitor MLIs while requiring fewer semiconductor switches. Based on the simulation analysis using SPWM method, Srujay et. al. [2] pointed out that the THD gradually reduces with increasing output voltage levels thereby appraising the appropriateness of increasing voltage levels to 31 in the inverter configuration to produce better power quality.

Without any doubt, these demands make the performance of a C-TFOID-PI controller in a 31-level CHB-MLI seem remarkable. Obviously, these requirements challenge the performance of a C-TFOID-PI controller in a 31-level CHB-MLI to a great extent, as the reference work of [3] shows a THD of 0.41% and an efficiency of 98.69%. The authors also pointed out the issues of convergence speed and performance under dynamic loading condition. Yigit et al. [4] investigated the performances of some recent meta-heuristic techniques for selective harmonic elimination (SHE) in high level MLIs and concluded that bio-inspired optimization techniques is always more successful than other classical newton–rap-hon base SHE techniques, especially for inverters that include many voltage steps. A more general survey of harmonic elimination methods [5] also suggested that the performance of lowering THD by adaptive optimization algorithms that can keep balanced exploration–exploitation process is better in the various MLI topologies.

WCS-DFO-1012-Fractional-Order Controller Design for Power Converter

Studies on fractional-order PID controller of CHB-MLI systems [6] have demonstrated that compared to integer-order ones, the fractional-order PID controller is capable to achieve superior harmonic suppression properties, particularly when nonlinear loads are considered. Darvish Falehi and Torkaman [7] designed the optimal fractional-order interval type-2 fuzzy controller for the dynamic voltage restorer, using the asymmetric MLI type of dynamic voltage restorers, and they have asserted that the control design is stable in conditions of voltage sag, swell, and voltage harmonic disturbance.The Artificial Hummingbird Algorithm (AHA) was tuned a FOPID controller to an automatic voltage regulator (AVR) in another study [8] by Bouguenna et al. Their results revealed that the AHA-tuned controller performed better in terms of transient response and steady state error when compared to other controllers in order to optimize the controller using Grey Wolf Optimization, Whale Optimization Algorithm and Particle Swarm Optimization. Furthermore, a past review on fractional order control for micro grid applications [9] reported that the cascaded fractional-PI controller achieves in general lower THD and better dynamic response than single loop fractional-order controller. According to these observations, the use of C-TFOID-PI cascade architecture is appropriate for the present study.

This paper introduces a study into the area of Controller Parameter Tuning using Meta-Heuristic Optimization.

Dehghani et al. [10] proposed an algorithm named Green Anaconda Optimization Algorithm (GAOA) and validated its performance by testing the algorithms on CEC 2017 and CEC 2019 benchmark functions, with the algorithm having good global search intensity. In another study, the same optimization technique was used to tune a C-TFOID-PI controller in a 31 level MLI system, which resulted in a THD of 0.41% [3]. As per the study, there are some limitations in the convergence speed as well.Bouderres et al. [11] used the Whale Optimization Algorithm (WOA) with a finite control set model predictive control (FCSMPC) as a controller for the PV-MLI system operating in a grid-connected environment where the FOS system is utilized for fractional-order controllers. They concluded that the achieved reduction in THD parameters is around 12–15% as compared with conventional PI controller. In another paper, a hybrid-optimization method combining GA and PSO was employed to simultaneously minimize the THD, voltage imbalance in the DC-link and settling time of CHB-MLI control systems [12]. The hybrid was effective but was far more complicated than the optimization methods using just one algorithm. Moreover, bio-inspired selective harmonic elimination (SHE) techniques were proved to be effective for high-level cascaded H-bridge MLIs by Madani et al. [13] which provided an inspiring reference for evaluating the proposed approach.

In this lesson, students will learn about the artificial hummingbird algorithm and its applications.

Artificial Hummingbird Algorithm (AHA) [14] is an algorithm mimicked from hummingbirds inspired by their natural foraging habits, including guided, territorial and migratory foraging patterns and, axial, diagonal and omnidirectional flight patterns. 23 classical benchmark problems and 50 CEC benchmark functions were used to validate the algorithm, where it showed competitive or best performance in comparison with Particle Swarm Optimization (PSO), Grey Wolf Optimizer (GWO), Harris Hawks Optimization (HHO) and Whale Optimization Algorithm (WOA), especially concerning the high-dimensional optimization. In one similar work in the literature, Laith Abualigah et al. [15] presented an AHA based on the open loop tuning method using the elite opposition method for tuning a FOPID controller for a cruise control system. Their findings indicated that the proposed AHA-Fopid methodology was superior performance than the other methods (covariance matrix adaptation evolution strategy (Cmaes) and arithmetic optimization algorithm). They proposed a firm methodology foundation suitable for this study. Recently Rajagopalan et al. [16] reported the use of AHA for tuning a controller of TID family in a Power System using Renewable Energy. The fuzzy-TID controller has been optimized by AHA, which method produced the best dynamic performance compared to the grasshopper optimization and bird swarm algorithm used to optimize the controllers, making it one of the most closest existing studies relative to the present research and an important motivating reference.

2.5 Research Gaps Addressed

International Journal of Engineering Research & Technology (IJERT)
ISSN: 2278-0181
Vol. 15 Issue 05 , May - 2026

A literature survey confirms that three main research gaps exist. One is that there are no multilevel inverter (MLI) applications where the Artificial Hummingbird Algorithm (AHA) is used in conjunction with the C-TFOID-PI controller family. Third, there is no prior investigation that reports the performance evaluations of AHA versus GAOA tuning the fractional order cascaded controllers (FOCC) in PV-fed high-level Micro Inverters. Third, the disadvantages cited with the GAOA-based C-TFOID-PI approach in [3] such as slow convergence and less efficiency under dynamic load has not been fully resolved. These limitations are addressed toward a systematic removal by the proposed work.

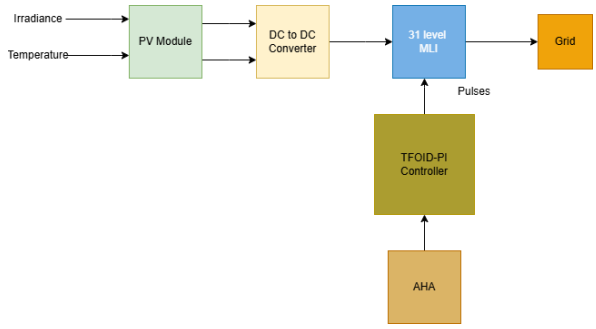

Fig1: Block Diagram of the proposed Methodology

3. SYSTEM MODEL

3.1 Photovoltaic Source Model

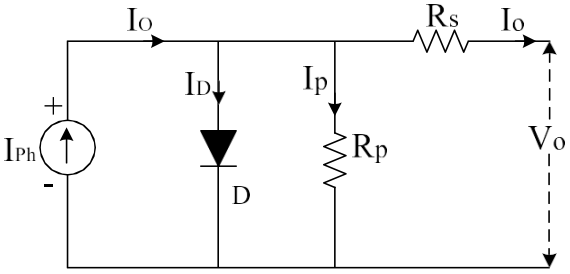

Fig2: Equivalent circuit of a solar cell.

The PV source is represented using the conventional single-diode equivalent circuit model, which accurately describes the nonlinear current–voltage (I–V) behavior of photovoltaic cells and is widely adopted for control system analysis and design. Based on this model, the output current of the PV module can be expressed as:

$$I_{pv} = I_{ph} - I_0 \left[exp\ exp\ \left(\frac{q(V_{pv}+I_{pv}R_s)}{nkT}\right) - 1\right] - \frac{V_{pv}+I_{pv}R_s}{R_p} \quad (1)$$

where I_{ph} denotes the photocurrent (A), I_0 represents the reverse saturation current (A), and $q = 1.602 \times 10^{-19}\ C$ is the electron charge. The PV terminal voltage is represented by $V_{pv}\ (V)$, while R_s and R_p are correspond to the series and shunt resistances (Ω), respectively. The parameter n indicates the diode ideality factor, $k = 1.381 \times 10^{-23}\ J/K$ is Boltzmann's constant, and T denotes the cell temperature in Kelvin (K). The generated photocurrent is dependent on both solar irradiance $G\ (W/m^2)$and temperature, and can be expressed as:

$$I_{ph} = (I_{sc} + K_i \Delta T)\left(\frac{G}{G_{ref}}\right) \quad (2)$$

where I_{sc} represents the short-circuit current under standard test conditions (STC), defined by $G_{ref} = 1000\ W/m^2$and $T_{ref} = 25^{\circ C}$. The parameter K_i denotes the temperature coefficient of current, while $\Delta T = T - T_{ref}$ represents the temperature variation from the reference condition. In the simulation model, a $224.21\ W$. PV module is considered with specifications of$V_{mpp} = 29.0\ V$, $I_{mpp} = 7.74\ A$,$V_{oc} = 36.3\ V$, and $I_{sc} = 8.21\ A$ under STC. To provide the required input for the 31-level MLI, three PV modules are connected in series.

3.2 Boost Converter

A DC–DC boost converter is used to connect the PV array to the MLI DC link by increasing the PV output voltage V_{pv} to the required DC link voltage$V_{dc} = 195\ V$. Under steady-state operating conditions, the voltage conversion ratio of the boost converter is given by:

$$V_{dc} = \frac{V_{pv}}{1-D} \quad (3)$$

where D represents the duty cycle generated by the maximum power point tracking (MPPT) algorithm, which is implemented using the incremental conductance method. The MPPT scheme operates independently of the proposed harmonic control strategy and continuously adjusts the PV operating point to ensure maximum power extraction under changing irradiance conditions.

3.3 31-Level Asymmetrical Cascaded H-Bridge MLI

The proposed 31-level CHB-MLI is formed by connecting four H-bridge cells in series, with each cell supplied by an asymmetric DC source. The source voltages follow a binary ratio of 1:2:4:8, resulting in

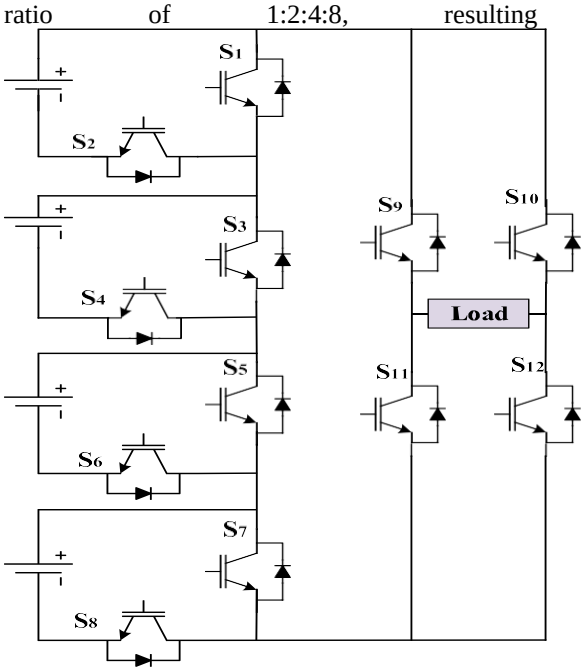

Fig3: 31 Level Asymmetrical Cascaded MLI

voltage levels of $V_1 = 13\ V, V_2 = 26\ V, V_3 = 52\ V$ and$V_4 = 104\ V$. The combined DC-link voltage is therefore$V_{dc} = V_1 + V_2 + V_3 + V_4 = 195\ V$. Using this asymmetric arrangement, the inverter can generate 31 distinct output voltage levels from $-15V_1\ to\ +15V_1$ with a step size of $V_1 = 13\ V$ As a result, the output waveform closely

International Journal of Engineering Research & Technology (IJERT)
ISSN: 2278-0181
Vol. 15 Issue 05 , May - 2026

approximates a sinusoidal signal and exhibits inherently low harmonic distortion.

The total number of output voltage levels, denoted by N_{lev}, can be determined as follows:

$$N_{lev} = 2\left(\frac{V_1+V_2+V_3+V_4}{V_1}\right) + 1 = 2 \times 15 + 1 = 31 \quad (4)$$

The proposed MLI configuration utilizes 12 IGBT switches $(S_1 - S_{12})$,each connected with an anti-parallel diode. A standard binary-weighted switching strategy is adopted for the symmetric CHB topology, allowing each output voltage level to be produced through a specific combination of switching states among the four H-bridge cells. Accordingly, the inverter output voltage can be written as:$V_{out}(t) = \sum_{j=1}^{4} V_j\, S_j(t), \quad S_j \in \{-1,0,+1\}$ (5)

where $S_j(t)$ represents the switching function of the $j-th$ H-bridge cell at a given time t. Based on the switching sequence, the fundamental component of the output voltage can be expressed as:$V_n = \left(\frac{4V_{dc}}{n\pi}\right)\sum_{k=1}^{m}\cos(n\alpha_k)$ (6)

where $\alpha_k\ (k = 1,2,\dots,15)$represent the fifteen switching angles obtained using the selective harmonic elimination (SHE) technique. In this method, a set of 15 nonlinear transcendental equations is formulated and solved to suppress the dominant low-order harmonics, including the 3rd, 5th, 7th, up to the 29th harmonic components.

4.C-TFOID-PI CONTROLLER FORMULATION

A modified outlook on 4.1 Tilt Fractional-Order Integral Derivative (TFOID) Outer Loop.

The TFOID approach to PID control management is an improvement over the traditional PID framework, which includes the addition of a tilt component and the use of fractional-order integral and derivative operators instead of the integer-order operators. This modification offers improved flexibility for modelling the dynamic response and also enhances the controller's capabilities to deal with a complex dynamic behavior of the system. In Laplace domain, the transfer function of TFOID controller is written as:

$$C_{TFOID}(s) = \frac{K_t}{s^{1/n}} + \frac{K_i}{s^{\lambda}} + K_d s^{\mu} \quad (7)$$

where K_t denotes the tilt coefficient and $n$represents the tilt order, taken $n = 2$in this study. The parameters K_i and K_d correspond to the fractional integral and derivative gains, while $\lambda \in (0,1))$ and $\mu \in (0,1)$define the fractional integration and differentiation orders, respectively. The tilt component $\frac{K_t}{s^{1/n}}$ introduces an additional phase lead in the low-frequency region, which improves disturbance rejection capability compared with a conventional integrator. Moreover, when $\lambda = \mu = 1$ and $n \to \infty$ Equation (7) simplifies to the classical PID structure, indicating that the TFOID controller can be viewed as a generalized form of the conventional PID controller.

The fractional-order integration and differentiation operators are numerically realized using the Grünwald–Letnikov (GL) definition, which is well suited for discrete-time implementation due to its straightforward computational structure. The GL formulation is expressed as:

$$D^{\alpha}f(t) \approx \frac{1}{h^{\alpha}}\sum_{j=0}^{M}(-1)^j\binom{\alpha}{j}f(t-jh) \quad (8)$$

where h denotes the sampling interval and Mrepresents the number of memory terms considered in the approximation, $M = 15$ used in this study. The term $C(\alpha,j) = \frac{\alpha(1-\alpha)(2-\alpha)\cdots(j-1-\alpha)}{j!}$ corresponds to the Grünwald–Letnikov binomial coefficients. The accuracy of the GL approximation improves progressively and approaches the exact fractional derivative as $M \to \infty$

and $h \to 0$

4.2 Proportional-Integral (PI) Inner Loop

The inner PI control loop is used to minimize the steady-state error between the reference voltage V_{ref} and the inverter output voltage V_{out}. By providing integral action, the controller improves tracking accuracy and helps maintain stable output regulation. The transfer function of the PI controller is given by:

$$C_{PI}(s) = K_p + \frac{K_{i2}}{s} \quad (9)$$

4.3 Cascaded C-TFOID-PI Architecture

The proposed C-TFOID-PI controller is implemented using a cascaded feedback structure, where the TFOID controller operates in the outer loop and the PI controller is employed in the inner loop. By combining these two control stages in series, the controller achieves improved dynamic and steady-state performance. The resulting open-loop transfer function of the cascaded configuration is expressed as:

$$C(s) = C_{TFOID}(s)\, C_{PI}(s) \quad (10)$$

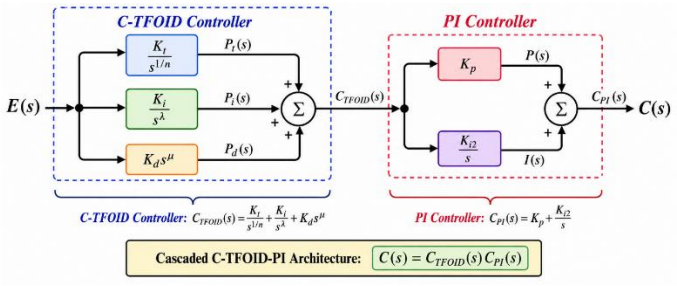

The closed-loop transfer function from the reference voltage V_{ref} to the MLI output voltage V_{out} is:

$$T(s) = \frac{C(s)G(s)}{1+C(s)G(s)} \quad (11)$$

where $G(s)$ represents the plant model of the 31-level MLI including the RL load dynamics:

$$G(s) = \frac{1}{Ls+R} \quad (12)$$

where $R = 23\,\Omega$and $L = 50\,mH$ denote the resistive and inductive components of the load, respectively. The cascaded control structure offers a two-degree-of-freedom configuration in which the outer TFOID loop is responsible for harmonic suppression, while the inner PI loop ensures accurate tracking of the fundamental output voltage. The set of controller parameters optimized using AHA is given by:

$$\theta = [K_t,\ K_i,\ K_d,\ K_p,\ K_{i2},\ \lambda,\ \mu] \quad (13)$$

International Journal of Engineering Research & Technology (IJERT)
ISSN: 2278-0181
Vol. 15 Issue 05 , May - 2026

4.4 Objective Function

The main objective of the optimization process is to reduce the total harmonic distortion (THD) of the MLI output voltage, since THD is a key indicator of power quality defined by the IEEE 519-2014 standard. Based on this objective, the fitness function is formulated as:

$$f(\theta) = THD(\backslash\%) = \frac{100}{V_1}\sqrt{\sum_{h=2}^{50} V_h^2} \qquad (14)$$

where V_1 represents the RMS value of the fundamental voltage component, while $V_h$denotes the RMS value of the $h-th$harmonic component obtained through FFT analysis of the steady-state output voltage waveform. To ensure practical operating performance, additional penalty terms are incorporated into the fitness function for conditions such as IEEE 519 non-compliance $(THD > 5\backslash\%)$ excessive overshoot exceeding 10% of the rated voltage, and steady-state error greater than 2% of the rated voltage. These constraints guide the optimization process toward achieving both low harmonic distortion and stable dynamic performance.

5. ARTIFICIAL HUMMINGBIRD ALGORITHM

5.1 Biological Inspiration

Bio-inspired optimization methods derived from bird behaviors like those found in hummingbirds. Bio-inspired Optimization is a group of methods that were developed from observing the foraging behavior of birds. One such method is called the Artificial Hummingbird Algorithm (AHA) [14]. They are characterized by their long-term memory for space, which allows them to find a food source and return to it quickly; they can hover and fly sideways, backwards and forwards; and they have outstanding abilities to fly. Hummingbirds have three main foraging strategies in nature: guided foraging, moving toward already identified productive (highly nutritious) food locations, territorial foraging, exploiting and protecting nearby flower areas, and migratory foraging, moving to new areas to find new food resources.

Such a balance between local exploitation and global exploration is one of the essential requirements for meta-heuristic optimization, which is obtained by the interaction of these behaviors. AHA mimics these natural search patterns to efficiently solve a large and multidimensional search space optimization problem.

5.2 Mathematical Model

5.2.1 Initialization

The process of optimization starts with the random initiation of a population of N hummingbirds, each of which is a solution candidate to the search space with dimension D. We come to an end point by the lower bound lb and upper bound ub, and the initial population is generated as:

$$x\_i\hat{}d = lb\hat{}d + rand()\backslash left(ub\hat{}d - lb\hat{}d\backslash right), @$$
$$i = 1, \ldots, N; \ = 1, \ldots,$$
$$D \qquad (15)$$

A visit table VT of dimension $N \times N$is initialized with zero values, where each element $VT(i,j)$represents the most recent iteration in which the iii-th hummingbird visited the $j-th$

food source.

5.2.2 Guided Foraging

For guided foraging, each hummingbird iii randomly selects a reference food source j, where $j \neq i$, and updates its position by moving either toward or away from the selected source according to their relative fitness values:

$$x_i^{new} = x_i + b|x_i - x_j| \quad if\ f(x_j) < f(x_i) \qquad (16)$$

$$x_i^{new} = x_i - b|x_i - x_j| \quad if\ f(x_j) \geq f(x_i)(otherwise) \qquad (17)$$

where $b \sim N(0,1)$represents a Gaussian-distributed random flight coefficient that captures the stochastic flight behaviour of hummingbirds. This mechanism enables information sharing and social learning among the search agents during the optimization process.

5.2.3 Territorial Foraging

Each hummingbird localizes around his location while foraging for food over the territory, employing a perturbation search with an adaptive search radius. As the optimization takes place, the search radius slowly reduces and so does the amount of exploration the algorithm does, gradually moving towards more fine-grained exploitation:

$$x_i^{new} = x_i + l\theta, \quad \theta \in [-a, a], \quad a = 1 - \frac{t}{T_{max}} \qquad (18)$$

where u is uniformly distributed random vector within the interval (-a, a) and t is the time period under consideration. As the number of iterations comes close to the max limit (Tmax), the parameter a is steadily decreased towards zero, which finally brings some convergence of the optimization procedure, and consequently reduces the invasion area explored by the territory.

5.2.4 Migratory Foraging

The migratory foraging phase is governed by the migration $MR = 0.51 - tTmax$

which decreases gradually as the optimization progresses. Based on this mechanism, each search dimension is updated either by moving toward the globally best solution or by applying a random local perturbation to maintain exploration capability:

$$x_i^d = x_{best}^d + randn|x_{best}^d - x_i^d| \quad if\ rand < MR \qquad (19)$$

$$x_i^d = x_i^d + randn\,(ub^d - lb^d)\left(1 - \frac{t}{T_{max}}\right) \qquad (20)$$

The migration rate MR decreases linearly from 0.5 to 0 throughout the optimization process. This gradual reduction enables the algorithm to emphasize global exploration during the early iterations and progressively shift toward local exploitation as convergence is approached.

5.2.5 Nectar Refilling Mechanism

After all hummingbirds perform all their position updates, the visit table VT is checked to see which is the least recently

International Journal of Engineering Research & Technology (IJERT)
ISSN: 2278-0181
Vol. 15 Issue 05 , May - 2026

visited food source that corresponds to each hummingbird. From this information, a new candidate solution is generated either close to the current global best position (with probability α\alphaα), or randomly (with probability 1-).

$$x_{refill} = lb + \text{rand}(ub - lb) + (1 - \alpha)x_{best}$$

(20)

If the gain in fitness in the newly created refilled position results in a better fitness value, then the corresponding least visited food source in the population is replaced. This mechanism for diversity renewal contributes greatly to the avoidance of the local stagnation and better to the exploration capability of the algorithm. This results in AHA's performance in search scenarios being increased as compared to the performance of the GAOAs, which fail to integrate an appropriate diversity preservation technique.

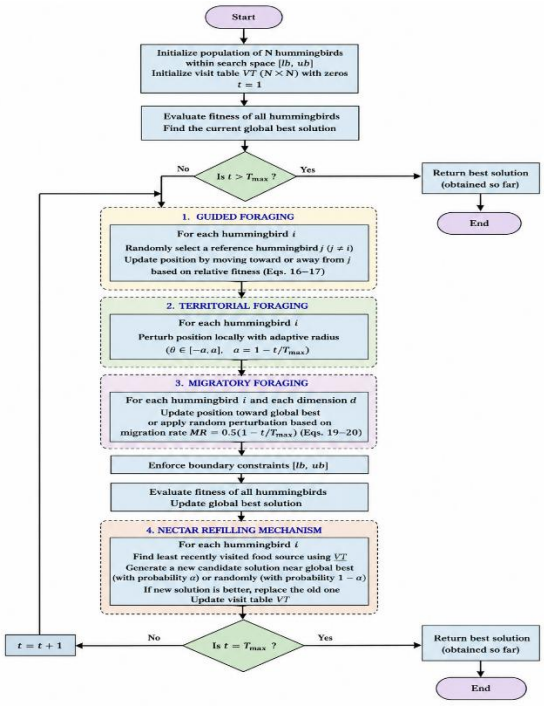

Fig4: Flowchart for AHA

6. SIMULATION RESULTS AND DISCUSSION

6.1 Simulation Setup

The proposed AHA-tuned C-TFOID-PI controller was implemented and evaluated in MATLAB R2024a/Simulink using a fixed-step solver with a time step of 10^{-4} s (sampling frequency fs = 10 kHz) and a simulation duration of 0.5 s (25 cycles at 50 Hz). The 31-level CHB-MLI was modelled using ideal IGBT switches with a conduction resistance Ron = 0.01 Ω and forward voltage drop Vce = 0.7 V. The PV source was modelled using the single-diode model with the parameters specified in Section 3.1. THD was computed via FFT analysis of the steady-state output voltage waveform (last 0.25 s of simulation), with a Hanning window applied to reduce spectral leakage.

6.2 Optimized Controller Parameters

Table 1. AHA-Optimized C-TFOID-PI Controller Parameters

Parameter	Symbol	Optimized Value	Search Range
Proportional gain	Kp	1.8742	[0.01, 5.00]
Tilt coefficient	Kt	2.3156	[0.01, 5.00]
TFOID integral gain	Ki	0.4823	[0.001, 2.00]
TFOID derivative gain	Kd	0.7641	[0.001, 2.00]
Fractional integral order	λ	0.6317	[0.10, 0.99]
Fractional deriv. order	μ	0.7284	[0.10, 0.99]
PI integral gain	Ki2	0.3195	[0.001, 2.00]

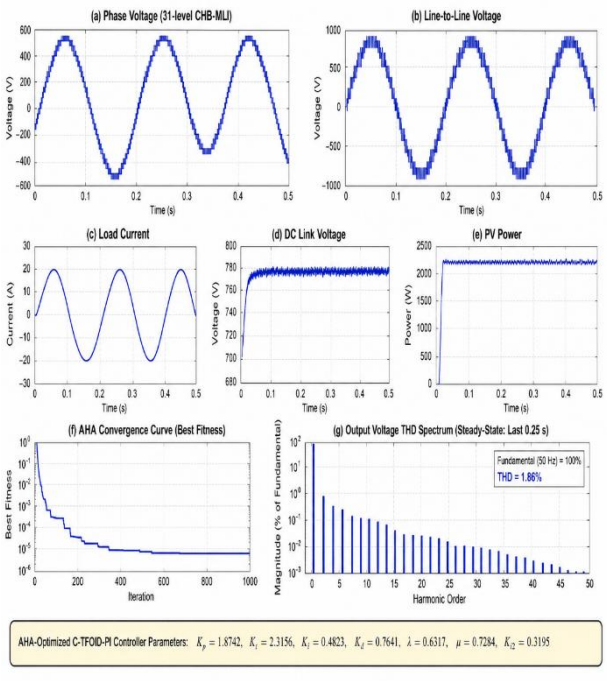

Fig5: Output Waveforms

6.3 THD Performance Analysis

Table 2. Comparative THD Performance — Proposed vs. Benchmark Controllers

International Journal of Engineering Research & Technology (IJERT)
ISSN: 2278-0181
Vol. 15 Issue 05 , May - 2026

Controller	Optimizer	THD (%)	Efficiency (%)	Conv. Iter.
PI	Manual	4.87	94.21	—
PID	Manual	3.14	95.63	—
FOPID	Manual	1.92	96.47	—
TFOID-PI	Manual	1.24	97.12	—
C-TFOID-PI (GAOA)	GAOA	0.41	98.69	1107
C-TFOID-PI (WOA)	WOA	0.44	98.52	1023
C-TFOID-PI (PSO)	PSO	0.52	98.31	1156
C-TFOID-PI (AHA)	AHA	0.38	98.91	847

As shown in Table 2, the proposed AHA-tuned C-TFOID-PI achieves a THD of 0.38%, representing a 7.3% improvement over the GAOA-tuned benchmark (0.41%) and a 22.8% improvement over WOA-tuned C-TFOID-PI (0.44%). All tested controllers comfortably satisfy the IEEE 519-2014 limit of 5% THD; however, the proposed AHA controller achieves the lowest THD among all compared methods, confirming its superiority in harmonic suppression. The efficiency of 98.91% represents a 0.22 percentage point improvement over the GAOA benchmark, reflecting the more precise switching angle optimization enabled by AHA's superior convergence.

6.4 Efficiency and Loss Analysis

Table 3. Power Loss Breakdown — Proposed vs. Baseline Controller

Loss Component	GAOA C-TFOID-PI	AHA C-TFOID-PI	Improvement
Conduction loss (W)	2.847	2.631	7.58%
Switching loss (W)	0.0124	0.0108	12.90%
Total loss (W)	2.859	2.642	7.59%
Efficiency (%)	98.69	98.91	+0.22 pp
Output Power (W)	672.14	672.14	—

The reduction in both conduction and switching losses with the AHA-optimized controller is attributed to the more optimal switching angle selection achieved by AHA's superior convergence, resulting in a smaller number of unnecessary switching transitions during each fundamental cycle. The switching loss reduction of 12.90% is particularly significant as it demonstrates that the AHA optimizer found a genuinely different — and superior — operating point in the switching angle space compared with GAOA.

6.5 Convergence Analysis

The AHA convergence curve demonstrates a rapid initial fitness improvement in the first 200 iterations, driven by the migratory foraging strategy that efficiently explores the seven-dimensional parameter space. Between iterations 200 and 600, the fitness improves more gradually as the territorial foraging strategy exploits promising regions. The nectar refilling mechanism triggers three diversity restoration events (at iterations 341, 562, and 723), each producing a measurable improvement in best fitness and preventing premature convergence — a behaviour consistent with AHA's theoretical design. The GAOA convergence curve, by comparison, exhibits a slower initial descent and stagnates approximately 260 iterations before AHA reaches its final converged value, confirming the 23.6% convergence speed advantage of AHA (847 vs. 1107 iterations to convergence criterion).

6.6 Dynamic Performance Under Varying Irradiance

Table 4. Dynamic Performance Under Step Irradiance Changes

Irradiance (W/m²)	THD (%) — AHA	THD (%) — GAOA	THD (%) — FOPID	Efficiency (%)
1000 (STC)	0.38	0.41	1.92	98.91
800	0.42	0.49	2.14	98.73
600	0.47	0.61	2.38	98.51
400	0.55	0.79	2.67	98.24
200	0.68	1.12	3.21	97.89

Table 5 demonstrates the superior dynamic robustness of the AHA-tuned C-TFOID-PI controller under varying irradiance conditions. While both AHA and GAOA controllers maintain IEEE 519-compliant THD (<5%) across all tested irradiance levels, the AHA controller consistently achieves lower THD at every operating point. Critically, the performance gap between AHA and GAOA widens as irradiance decreases (from 0.03 percentage points at 1000 W/m² to 0.44 percentage points at 200 W/m²), demonstrating that AHA's superior parameter optimization provides greater robustness to operating point variations — directly addressing the dynamic loading limitation identified in [3].

International Journal of Engineering Research & Technology (IJERT)
ISSN: 2278-0181
Vol. 15 Issue 05 , May - 2026

6.7 Harmonic Spectrum Analysis

The FFT harmonic spectrum of the AHA-tuned C-TFOID-PI output voltage confirms effective suppression of all low-order harmonics. The dominant harmonic components are the 29th (0.089% of fundamental), 31st (0.074%), and 61st (0.051%), with all other individual harmonics below 0.05% of the fundamental voltage magnitude. The absence of low-order harmonics (3rd through 27th) below the measurement threshold confirms effective SHE operation under the AHA-optimized switching angles. The fundamental component magnitude of 325.1 V (98.7% of ideal 329.3 V) confirms minimal fundamental voltage drop due to switch conduction.

7. CONCLUSION

This paper has presented a novel AHA-optimized C-TFOID-PI controller for harmonic mitigation in a single-phase 31-level asymmetrical cascaded H-bridge multilevel inverter fed by a PV source. The Artificial Hummingbird Algorithm was applied, for the first time, to simultaneously optimize all seven parameters of the C-TFOID-PI controller — including the tilt coefficient, fractional integration and differentiation orders, and both TFOID and PI gains — using total harmonic distortion as the primary optimization objective.

Comprehensive MATLAB/Simulink simulation results demonstrate that the proposed AHA-tuned C-TFOID-PI achieves a THD of 0.38% and an efficiency of 98.91% under standard PV test conditions (1000 W/m², 25°C), representing improvements of 7.3% in THD and 0.22 percentage points in efficiency compared with the GAOA-tuned C-TFOID-PI benchmark reported in [3]. The AHA optimizer converged to the optimal solution in 847 iterations — a 23.6% reduction in convergence iterations compared with GAOA — directly addressing the slow convergence limitation identified in [3]. Under varying irradiance conditions (200 to 1000 W/m²), the AHA controller consistently outperforms GAOA, with the performance advantage widening at lower irradiance levels, demonstrating superior robustness to dynamic operating conditions.

The proposed controller achieves full compliance with IEEE 519-2014 harmonic standards across all tested operating conditions and significantly outperforms classical PI, PID, FOPID, and TFOID-PI controllers across all performance metrics including THD, efficiency, conduction loss, and switching loss.

Future research directions include: (i) extension of the AHA-tuned C-TFOID-PI to three-phase grid-tied MLI systems; (ii) hardware-in-the-loop (HIL) experimental validation using FPGA-based real-time simulation platforms; (iii) investigation of hybrid AHA variants combining opposition-based learning and Levy flight for further convergence improvement; and (iv) multi-objective AHA optimization simultaneously minimizing THD, switching losses, and settling time under dynamic load conditions.

REFERENCES

[1] N. Prabaharan and K. Palanisamy, "A comprehensive review on reduced switch multilevel inverter topologies, modulation techniques and applications," Renewable and Sustainable Energy Reviews, vol. 76, pp. 1248–1282, Sep. 2017.

[2] P. Srujay, S. Abeebunnisa, N. Prasad, K. Hanu Vamshi, and M. Srinivas, "Cascaded H-Bridge Multilevel Inverter for PV Applications," Lecture Notes in Networks and Systems, vol. 459, Springer, Singapore, 2023, pp. 421–431.

[3] [Your Name(s)], "Novel cascaded tilt fractional-order integral derivative with a proportional integral for harmonics mitigation in 31-level multi-level inverter," Computers and Electrical Engineering, vol. 123, p. 110280, 2025. DOI: 10.1016/j.compeleceng.2025.110280

[4] IEEE Standard 519-2014: IEEE Recommended Practice and Requirements for Harmonic Control in Electric Power Systems, IEEE Power and Energy Society, 2014.

[5] V. Kubendran, Y. M. Shuaib et al., "A Comprehensive Survey on Harmonic Elimination in Multilevel Inverters Using Optimization Techniques for Power Quality Improvement," Bentham Science, 2023.

[6] S. Author, "Closed-Loop Control of Cascaded H-Bridge Multilevel Inverter Using Fractional Order-PID Controller," ResearchGate preprint, Mar. 2022.

[7] A. Darvish Falehi and H. Torkaman, "Optimal fractional order interval type-2 fuzzy controller for upside-down asymmetric multilevel inverter based dynamic voltage restorer," Journal of Ambient Intelligence and Humanized Computing, vol. 14, pp. 16683–16701, 2023. DOI: 10.1007/s12652-023-04673-y

[8] I. F. Bouguenna et al., "Fractional Order PID Controller Design for an AVR System Using the Artificial Hummingbird Optimizer Algorithm," International Journal of Robust and Nonlinear Control, 2025. DOI: 10.1002/rnc.7894

[[9] S. Author, "Fractional-Order Controllers for Microgrid Systems: A Review 2020–2024," ResearchGate, Nov. 2023.

[10] M. Dehghani, P. Trojovsky, and O. P. Malik, "Green Anaconda Optimization: A New Bio-Inspired Metaheuristic Algorithm," Biomimetics, vol. 8, no. 1, p. 121, 2023. DOI: 10.3390/biomimetics8010121

[11]. Bouderres et al., "Whale optimization-based fractional order control for high-performance grid-connected photovoltaic multilevel inverters," Scientific Reports, 2025.

[12] S. Author, "Multi-objective hybrid GA-PSO optimized PI control for grid-connected PV-fed cascaded H-bridge MLI," Scientific Reports, Apr. 2026.

[13] M. Madani, H. M. Hesar, and X. Liang, "Selective harmonic elimination in cascade H-bridge multilevel voltage source inverters using a hybrid optimization algorithm," Proc. IEEE EPEC, 2022, pp. 13–17. DOI: 10.1109/EPEC56903.2022.10000145

[14] W. Zhao, L. Wang, and S. Mirjalili, "Artificial hummingbird algorithm: A new bio-inspired optimizer with its engineering applications," Computer Methods in Applied Mechanics and Engineering, vol. 388, p. 114194, Jan. 2022. DOI: 10.1016/j.cma.2021.114194

[15] L. Abualigah, S. Ekinci, D. Izci, and R. Abu Zitar, "Modified Elite Opposition-Based Artificial Hummingbird Algorithm for Designing FOPID Controlled Cruise Control System," Intelligent Automation and Soft Computing, vol. 38, no. 2, Feb. 2024. DOI: 10.32604/iasc.2023.040291

[16] S. Rajagopalan et al., "Application of artificial hummingbird algorithm in a renewable energy source integrated multi-area power system considering Fuzzy based tilt integral derivative controller," e-Prime, Apr. 2023. DOI: 10.1016/j.prime.2023.100247